

PERFORMANCE ANALYSIS OF MULTIPLE-SCAN DETECTION IN HEAVY HETEROGENEOUS SEA CLUTTER

S. J. Chen, L. J. Kong^{*}, and J. Y. Yang

School of Electronic Engineering, University of Electronic Science and Technology of China, Chengdu, Sichuan 611731, China

Abstract—Traditional detection approaches for the dim moving target are addressed under the background of homogeneous sea clutter. However, the realistic clutter commonly appears inhomogeneous, resulting in the low detectability. A heterogeneous multiple-scan detection framework is described in this paper, which combines the inhomogeneous coherent integration in the dwell of single scan and the non-coherent integration of the results from single-scan process across the multiple scans. In the inhomogeneous coherent integration, the Heterogeneous Single-scan Coherent Detector (HSCD) is derived, resorting to the two-step Generalized Likelihood Ratio Test (GLRT) criterion and a hybrid covariance matrix estimation scheme, where the nonhomogeneous Kelly detector and the inhomogeneous Adaptive Matched Filter (AMF) are also considered. Additionally, the Viterbi-Like (VL) algorithm is employed as the non-coherent integration strategy. Finally, the numerical simulations with Monte Carlo method analyze the performance of the nonhomogeneous multiple-scan detectors under amplitude and distribution clutter heterogeneity.

1. INTRODUCTION

Detection for slowly moving targets in heavy noise environment is considered as a challenging problem in many applications, including optics, sonar and radar [1–3]. Classically, the broad-sense noise may contain thermal noise, clutter, and possibly jamming. Concretely the heavy clutter in the oceanic environment, illuminated by High-Resolution (HR) radar system [4–6] where the conventional Gaussian or Rayleigh model is no longer met, causes the unacceptable performance

Received 28 June 2012, Accepted 16 August 2012, Scheduled 20 August 2012

* Corresponding author: Ling Jiang Kong (lingjiang.kong@gmail.com).

degradation, and thereby many multiple-scan methods are proposed in the literatures for the purpose of improving the detectability for dim targets. The multiple-scan signal averaging method is provided to diminish noise (not clutter), leading the improvement of both Signal-to-Noise Ratio (SNR) and detection performance [7]. The researchers address the effect of the scan rate on the detection performance with the scan-to-scan processors in approximate Gaussian clutter [8, 9]. Recently, a multiple-scan application, so-called Radon transform, is presented to test against the HR sea-clutter data [10].

However, these mentioned methods concentrate on the homogeneous assumption for the sea background, and the inhomogeneous environments with unknown covariance matrices are more commonly encountered. The heterogeneity is generally with respect to inhomogeneous reflectivity (e.g., amplitude and/or spectral variation, clutter edges, moving discretets) in reality [11]. Therefore, the heterogeneous clutter model is deemed to be more suitable for non-flat areas [12, 13]. Precisely in HR radar system, an attempt to take into account non-homogeneity is to assume that the primary and secondary data samples share the same covariance matrix structure up to an unknown scaling factor, so-called partially homogeneous [14]. A more widely used and physically motivated model for nonhomogeneous clutter is the compound-Gaussian model [15]. In practical, it is great potential to exhibit various heterogeneous clutter models for complicated and inhomogeneous sea clutter, and unfortunately there does not yet exist a specific multiple-scan method to process this case of heterogeneous sea clutter.

Therefore, a heterogeneous multiple-scan detection framework is described in this paper. It is to detect the existence of weak target embed in the Cell Under Test (CUT) with the decision scheme, which combines the inhomogeneous coherent integration in the dwell of single scan and the non-coherent integration of the results from single-scan process across the multiple scans. In the inhomogeneous coherent integration, the Heterogeneous Single-scan Coherent Detector (HSCD) is provided, according to the two-step Generalized Likelihood Ratio Test (GLRT) criterion. At the same time, for the purpose of comparison, the Adaptive Matched Filter (AMF) and Kelly detector with a Hybrid estimate scheme of covariance matrix, also referred to as components of multiple-scan detectors, namely HAMF and HKelly respectively, are considered as the heterogeneous coherent processors. Precisely, the hybrid covariance matrix estimator can be capable of adapting the nonhomogeneous sea clutter with unknown Power Spectrum Density (PSD). In the non-coherent integration, the procedure, namely the Viterbi-Like (VL) method [16], based upon the

Viterbi algorithm [17], is the reduced-complexity and power-efficient methodology of best searching weak moving target in the trellis.

Therefore, under this framework, the three heterogeneous multiple-scan detectors are provided, including the VL-HSCD, VL-HAMF and VL-HKelly consisted of VL method and HSCD, HAMF, HKelly, respectively. Finally, we address the analysis in the performance assessment of the detectors (VL-HSCD, VL-HAMF, and VL-HKelly) for different target types including both Swerling 0 and Swerling 1 [18] and various nonhomogeneous scenarios, especially amplitude-heterogeneity and distribution-heterogeneity using the Monte Carlo method.

The paper is organized as follows. Section 2 contains the signal models of both the target and heterogeneous sea clutter. The inhomogeneous multiple-scan detector is introduced in Section 3. In Section 4, the numerical simulation results are presented with Monte Carlo. And the conclusions are provided in Section 5.

2. SIGNAL MODEL

In this paper, we assume that the radar transmits a coherent train of N Coherent Processing Interval (CPI) pulses in single scan and that the receiver properly demodulates filters and samples the incoming waveform. The observation vector $z_{l_s} \in C^{N \times 1}$ (C being the complex field), mutually independent between scans, is corresponded to the output of the l th range cell and the s th azimuth cell, given by

$$z_{l_s} = [z_{l_s}(1), z_{l_s}(2), \dots, z_{l_s}(N)]^T \in C^{N \times 1} \quad (1)$$

where $(\cdot)^T$ denotes the transposition operation. Then the problem of detecting a target that occupies in the l_k th range cell and s_k th azimuth cell of the k th scan ($k = 1, \dots, K$) can be formulated in terms of the following binary hypothesis test without loss of generality:

$$\begin{aligned} H_0 : z_{l_k s_k} &= \mathbf{c}_{l_k s_k}, \quad l \in \{1, \dots, L\}, \quad s \in \{1, \dots, S\} \\ H_1 : \begin{cases} z_{l_k s_k} = a_{l_k s_k} \mathbf{p}_{l_k s_k} + \mathbf{c}_{l_k s_k}, & l = l_k \in \{1, \dots, L\}, \quad s = s_k \in \{1, \dots, S\} \\ z_{l_k s_k} = \mathbf{c}_{l_k s_k}, & l \in \{1, \dots, L\} \setminus \{l_k\}, \quad s \in \{1, \dots, S\} \setminus \{s_k\} \end{cases} \end{aligned} \quad (2)$$

where $a_{l_k s_k}$ denotes the unknown parameter, accounting for the target and the channel propagation effects, and $\mathbf{p}_{l_k s_k}$ indicates the known steering vector. The clutter $\mathbf{c}_{l_k s_k}$ is modeled as the compound-Gaussian vector according to both the theoretical modeling of sea backscatter [19] and the statistical analysis of the recorded live data of HR sea clutter [20], which can be mathematically described as Spherically Invariant Random Process (SIRP) of the produce of two

components, texture and speckle, represented as

$$\mathbf{c}_{l_k s_k} = \zeta_{l_k s_k} \mathbf{x}_{l_k s_k} \quad (3)$$

with the covariance matrices $\mathbf{M}_{l_k s_k} = E[\mathbf{c}_{l_k s_k} \mathbf{c}_{l_k s_k}^H]$ and $\mathbf{M}_{X_{l_k s_k}} = E[\mathbf{x}_{l_k s_k} \mathbf{x}_{l_k s_k}^H]$, where $(\cdot)^H$ denotes conjugate transpose of the argument and $E[\cdot]$ is the statistical expectation. The speckle $\mathbf{x}_{l_k s_k}$ is a complex, circle, zero mean stationary Gaussian vector with covariance matrix $\mathbf{M}_{X_{l_k s_k}}$, and the texture $\zeta_{l_k s_k}$ is a nonnegative real stochastic variable and its distribution is commonly determined by some parameters.

In heterogeneous environment, especially amplitude-heterogeneous condition, the power in each resolution cell of clutter is assumed to be various, particularly the case of partially homogeneous environment. In the situation of distribution-heterogeneity, one case is that the parameters of the distribution of texture component are not the same in test and training samples. Another case is that the PSD of speckle component is changed in every clutter cell, also referred to as spectral heterogeneity.

3. NONHOMOGENEOUS MULTIPLE-SCAN DETECTOR

The problem of detecting a radar target of interest in a clutter-dominated environment can be posed in terms of the binary hypothesis test (2). Typically, the optimum solution to the problem (2) is to determine the likelihood ratio test in the Neyman-Pearson sense, given the prior knowledge of both the parameter $a_{l_k s_k}$ and the clutter covariance matrix $\mathbf{M}_{l_k s_k}$. However, the prior information is commonly unknown in practice. Hence, GLRT criterion is employed as the suitable mean to circumvent the drawback of the prior uncertainty.

For the case at hand, the canonical GLRT detection strategy yields

$$\Lambda(\mathbf{Z}) = \max_{D \in S_{ka}, a_{l_1 s_1}, \dots, a_{l_K s_K}} \frac{\max_{\mathbf{M}_{l_1 s_1}, \dots, \mathbf{M}_{l_K s_K}} f_{H_1}}{\max_{\mathbf{M}_{l_1 s_1}, \dots, \mathbf{M}_{l_K s_K}} f_{H_0}} \frac{H_1}{H_0} \gtrsim \gamma \quad (4)$$

where

$$f_{H_1} = f(\mathbf{Z} | \mathbf{M}_{l_1 s_1}, \dots, \mathbf{M}_{l_K s_K}, a_{l_1 s_1}, \dots, a_{l_K s_K}, H_1) \quad (5)$$

$$f_{H_0} = f(\mathbf{Z} | \mathbf{M}_{l_1 s_1}, \dots, \mathbf{M}_{l_K s_K}, H_0) \quad (6)$$

with $\mathbf{Z} = \{z_{l_1 s_1}, \dots, z_{l_K s_K}\}$, where $D = \{(l_1, s_1), \dots, (l_K, s_K)\} \in S_{ka}$ is the sequence of points occupied by a prospective target in the searching domain, and γ is the detection threshold to be set according to the desired value of the probability of false-alarm (P_{fa}).

At the design stage, considering the mutual independence of the signal $z_{l_k s_k}$ between scans, and after some algebra, the test (4) can be substituted as

$$\begin{aligned} \Lambda(\mathbf{Z}) &= \max_{D \in S_{ka}} \sum_{k=1}^K \ln \frac{\max_{\mathbf{M}_{l_k s_k}, a_{l_k s_k}} f(z_{l_k s_k} | \mathbf{M}_{l_k s_k}, a_{l_k s_k}, H_1)}{\max_{\mathbf{M}_{l_k s_k}} f(z_{l_k s_k} | \mathbf{M}_{l_k s_k}, H_0)} \\ &= \max_{D \in S_{ka}} \sum_{k=1}^K \ln \Lambda(z_{l_k s_k}) \underset{H_0}{\overset{H_1}{\geq}} \gamma_1 \end{aligned} \quad (7)$$

where γ_1 is used for the appropriate modification of the original threshold in (4), and $\Lambda(z_{l_k s_k})$, such as HSCD, HAMF or HKelly, is deemed as the test statistic of the k th scan. Moreover, VL algorithm is introduced to choose the trajectory D of possible target and to realize the maximization of the multiple-scan decision function (7).

3.1. Heterogeneous Signal-scan Coherent Detector (HSCD)

As discussed before, the sea clutter is modeled as the compound-Gaussian process, which can be mathematically described as a significant simplification of SIRP specified based upon a first- and second-order characterization only [21]. More precisely, the clutter $\mathbf{c}_{l_k s_k}$ is a zero-mean wide-sense stationary stochastic process, and considering the expression (3), its N -order Probability Density Function (PDF) is shown as

$$f_{\mathbf{c}_{l_k s_k}}(\mathbf{c}_{l_k s_k}) = \frac{1}{\pi^N \|\mathbf{M}_{X_{l_k s_k}}\|} h_N \left(\mathbf{c}_{l_k s_k}^H \mathbf{M}_{X_{l_k s_k}}^{-1} \mathbf{c}_{l_k s_k} \right) \quad (8)$$

and

$$h_N \left(\mathbf{c}_{l_k s_k}^H \mathbf{M}_{X_{l_k s_k}}^{-1} \mathbf{c}_{l_k s_k} \right) = \int_0^\infty \zeta_{l_k s_k}^{-2N} \exp \left(- \frac{\mathbf{c}_{l_k s_k}^H \mathbf{M}_{X_{l_k s_k}}^{-1} \mathbf{c}_{l_k s_k}}{\zeta_{l_k s_k}^2} \right) f(\zeta_{l_k s_k}) d\zeta_{l_k s_k} \quad (9)$$

where $\|\cdot\|$ denotes the determinant of a square matrix.

Combining the Equations (8) and (9), $\Lambda(z_{l_k s_k})$ can be expressed as

$$\Lambda(z_{l_k s_k}) = \max_{a_{l_k s_k}} \frac{\max_{\mathbf{M}_{X_{l_k s_k}}} \int_0^\infty \zeta_{l_k s_k}^{-2N} \exp \left(- \frac{\Omega_1(l_k s_k)}{\zeta_{l_k s_k}^2} \right) f(\zeta_{l_k s_k}) d\zeta_{l_k s_k}}{\max_{\mathbf{M}_{X_{l_k s_k}}} \int_0^\infty \zeta_{l_k s_k}^{-2N} \exp \left(- \frac{\Omega_0(l_k s_k)}{\zeta_{l_k s_k}^2} \right) f(\zeta_{l_k s_k}) d\zeta_{l_k s_k}} \quad (10)$$

where

$$\Omega_1(l_k s_k) = (z_{l_k s_k} - a_{l_k s_k} \mathbf{p}_{l_k s_k})^H \mathbf{M}_{X_{l_k s_k}}^{-1} (z_{l_k s_k} - a_{l_k s_k} \mathbf{p}_{l_k s_k}) \quad (11)$$

$$\Omega_0(l_k s_k) = z_{l_k s_k}^H \mathbf{M}_{X_{l_k s_k}}^{-1} z_{l_k s_k} \quad (12)$$

Obviously, it is difficult to implement the integration of the detector (10) without special $f(\zeta_{l_k s_k})$. Consequently, K -distributed clutter [22] with the modulating variate $\zeta_{l_k s_k}$, as the most popular model for compound-Gaussian clutter, is taken into account in this paper for two reasons: physical plausibility and mathematical convenience, while the PDF of $f(\zeta_{l_k s_k})$ is a generalized Gamma distribution, shown as

$$f(\zeta_{l_k s_k}) = \frac{b}{2^{v-1} \Gamma(v)} (b \zeta_{l_k s_k})^{2v-1} \exp\left(-\frac{b^2 \zeta_{l_k s_k}^2}{2}\right) \quad (13)$$

where v and b denote the shape and scale parameter respectively with $b = \sqrt{2v}$.

Subsequently, the expression (9) under K -distributed clutter yields

$$\begin{aligned} & h_N \left(\mathbf{c}_{l_k s_k}^H \mathbf{M}_{X_{l_k s_k}}^{-1} \mathbf{c}_{l_k s_k} \right) \\ &= \frac{b^{v+N} \left(\mathbf{c}_{l_k s_k}^H \mathbf{M}_{X_{l_k s_k}}^{-1} \mathbf{c}_{l_k s_k} \right)^{\frac{v-N}{2}}}{2^{v-1} \Gamma(v)} K_{N-v} \left(b \sqrt{\mathbf{c}_{l_k s_k}^H \mathbf{M}_{X_{l_k s_k}}^{-1} \mathbf{c}_{l_k s_k}} \right) \end{aligned} \quad (14)$$

with the modified second-kind Bessel function $K_{N-v}(\cdot)$ and the Eulerian Gamma function $\Gamma(\cdot)$.

The Equation (10) at the case can be expressed as

$$\Lambda(z_{l_k s_k}) = \frac{\max_{a_{l_k s_k}, \mathbf{M}_{X_{l_k s_k}}} \Omega_1(l_k s_k)^{\frac{v-N}{2}} K_{N-v} \left(b \sqrt{\Omega_1(l_k s_k)} \right)}{\max_{\mathbf{M}_{X_{l_k s_k}}} \Omega_0(l_k s_k)^{\frac{v-N}{2}} K_{N-v} \left(b \sqrt{\Omega_0(l_k s_k)} \right)} \quad (15)$$

The reference [23] shows that it is difficult to jointly maximize with respect to $a_{l_k s_k}$ and unknown $\mathbf{M}_{X_{l_k s_k}}$, and a closed-form solution is nonexistent. In order to overcome the drawback, we resort to the two-step GLRT design procedure.

Step 1: we derive the detector (15) assuming that the structure of covariance matrix is known, and thereby we can obtain the Maximum Likelihood Estimation (MLE) of $a_{l_k s_k}$, shown as

$$\hat{a}_{l_k s_k} = \frac{\mathbf{p}_{l_k s_k}^H \mathbf{M}_{X_{l_k s_k}}^{-1} z_{l_k s_k}}{\mathbf{p}_{l_k s_k}^H \mathbf{M}_{X_{l_k s_k}}^{-1} \mathbf{p}_{l_k s_k}} \quad (16)$$

Under the condition of high sea-state where the value of v is small ($v \rightarrow 0.1$), as well as considering the scale parameter $b = \sqrt{2v}$, the modified second-kind Bessel function can admit the asymptotic development

$$K_{N-v}(\mu) \approx \frac{\Gamma(N-v)}{2} \left(\frac{2}{\mu}\right)^{N-v} \quad (17)$$

Combining the Equations (13), (16) and (17), the decision function $\Lambda(z_{l_k s_k})$ of HSCD can be expressed as

$$\Lambda(z_{l_k s_k}) \approx \frac{z_{l_k s_k}^H \mathbf{M}_{X_{l_k s_k}}^{-1} z_{l_k s_k} \mathbf{P}_{l_k s_k}^H \mathbf{M}_{X_{l_k s_k}}^{-1} \mathbf{P}_{l_k s_k}}{z_{l_k s_k}^H \mathbf{M}_{X_{l_k s_k}}^{-1} z_{l_k s_k} \mathbf{P}_{l_k s_k}^H \mathbf{M}_{X_{l_k s_k}}^{-1} \mathbf{P}_{l_k s_k} - \left| \mathbf{P}_{l_k s_k}^H \mathbf{M}_{X_{l_k s_k}}^{-1} z_{l_k s_k} \right|^2} \quad (18)$$

where $|\cdot|$ denotes the modulus of a complex number.

Step 2: the true covariance matrix $\mathbf{M}_{X_{l_k s_k}}$ is substituted for its estimate resorting to the suitable method. In this paper, the hybrid method [24], employing both the primary and secondary data, can be capable of estimating the unknown covariance matrix $\mathbf{M}_{X_{l_k s_k}}$ under various conditions of inhomogeneous clutter. Firstly, we assume two independent data sets: the primary data set $(\mathbf{B}_{pr})_{l_k s_k}$ of size $N \times J_T$ extracted from the CUT and the secondary data set $(\mathbf{B}_{se})_{l_k s_k}$ of size $N \times J_t$ drawn from adjacent range gates around CUT. Furthermore, define the combined data set $\mathbf{B}_{l_k s_k} = [(\mathbf{B}_{pr})_{l_k s_k}, (\mathbf{B}_{se})_{l_k s_k}]$ of the size $N \times J$ with $J = J_T + J_t$, and $(\mathbf{t}_{J_T})_{l_k s_k} = [e^{j\phi_1}, \dots, e^{j\phi_{J_T}}]_{l_k s_k}^T$ denotes a length J_T vector containing the initial phases $\phi_1, \dots, \phi_{J_T}$. Finally, the covariance matrix $\mathbf{M}_{X_{l_k s_k}}$ can be expressed in terms of the primary and secondary data covariances matrices estimates $\Xi_{l_k s_k} = \frac{1}{J_T-1} [(\mathbf{B}_{pr})_{l_k s_k} (\mathbf{B}_{pr})_{l_k s_k}^H - \mathbf{r}_{l_k s_k} \mathbf{r}_{l_k s_k}^H]$ and $\Theta_{l_k s_k} = \frac{1}{J_t} (\mathbf{B}_{se})_{l_k s_k} (\mathbf{B}_{se})_{l_k s_k}^H$, shown as

$$\mathbf{M}_{X_{l_k s_k}} = \frac{1}{J_T + qJ_t - 1} [(J_T - 1)\Xi_{l_k s_k} + qJ_t\Theta_{l_k s_k}] \quad (19)$$

with $\mathbf{r}_{l_k s_k} = \mathbf{B}_{l_k s_k} \mathbf{t}_{l_k s_k}^*$ where $\mathbf{t}_{l_k s_k} = \frac{1}{J_T} [(\mathbf{t}_{J_T})_{l_k s_k}^T, \mathbf{0}_{J_t \times 1}^T]^T$ and the conjugated operator $(\cdot)^*$. The parameter q scales the contribution of the secondary data depending on the degree of heterogeneity ($0 \leq q \leq 1$). In reality, the secondary samples would most likely exhibit different degrees of heterogeneity. Lumping the entire training data into the covariance matrix $\Theta_{l_k s_k}$ prior to the non-homogeneity detection can, for instance, lead to the entire set being discarded as a result of the highly biased data. Hence, the expression (19) is somewhat basic and inflexible.

In order to consider the degree of heterogeneity of each training sample, the inhomogeneous measure matrix $\mathbf{Q}_{l_k s_k}$ is given by $\mathbf{Q}_{l_k s_k} =$

$$\begin{bmatrix} \mathbf{I}_{J_T \times J_T} & \mathbf{0}_{J_T \times J_t} \\ \mathbf{0}_{J_t \times J_T} & \text{diag}(\mathbf{q})_{J_t \times J_t} \end{bmatrix}_{l_k s_k}$$
 where the operation $\text{diag}(\mathbf{q})_{J_t \times J_t}$ forms a matrix with the elements of \mathbf{q} placed on the diagonal and off-diagonal elements equal to 0, and $\mathbf{I}_{J_T \times J_T}$ is the $J_T \times J_T$ unit matrix. Specially, the elements q_{J_i} , $J_i = J_1, \dots, J_t$ in the matrix $\text{diag}(\mathbf{q})_{J_t \times J_t}$ employ the same definition as the parameter q and $0 \leq q_{J_i} \leq 1$. The Generalized Inner Product (GIP) method [25] or the prior information of topography can decide the value of q_{J_i} . The hybrid covariance matrix estimate $\mathbf{M}_{X_{l_k s_k}}$ with generalized variable scale can then be rewritten as

$$\mathbf{M}_{X_{l_k s_k}} = \frac{1}{\text{tr}(\mathbf{Q}_{l_k s_k}) - 1} \left[\mathbf{B}_{l_k s_k} \mathbf{Q}_{l_k s_k} \mathbf{B}_{l_k s_k}^H - \mathbf{r}_{l_k s_k} \mathbf{r}_{l_k s_k}^H \right] \quad (20)$$

Relevant to our scope, the hybrid method turns out to achieve the asymptotically Constant False Alarm Rate (CFAR) [24].

3.2. Viterbi-like (VL) Algorithm

The Viterbi algorithm is an established optimization technique for discrete Markovian systems, extensively used in telecommunications and speech recognition. In practice, it is essentially a batch algorithm of a fixed-lag processing mode for merging of paths in the trellis with the physically admissible state transitions stored in the processor. The modified Viterbi algorithm, namely the VL algorithm, processes the entirely potential trajectories of the slowly moving target in the slow scan HR radar typically operating with scanning rates of about 6–60 rpm [9], illustrated in Figure 1.

The VL algorithm is utilized as the non-coherent integration scheme, and the iterative equation of the algorithm can be used to handle the possible path of the target in the test (7), shown as

$$d(k) = \max u(k-1, k) + d(k-1) \quad (21)$$

where $u(k-1, k)$ is the incremental or transition cost of the target from the $(k-1)$ th scan to the k th scan which is the nonlinear logarithm operation of the transition probability, and $d(k)$ can be stated as the cumulative or path cost, which is also done the nonlinear operation to the maximum of the likelihood function of the path [26].

Hence, the test (7) turns into

$$\begin{cases} \Lambda(\mathbf{Z}) = d(K) \geq \gamma \\ d(k) = d(k-1) + \max\{\ln[\Lambda(z_{l_k s_k})]\}_g, \quad k = 2, \dots, K \end{cases} \quad (22)$$

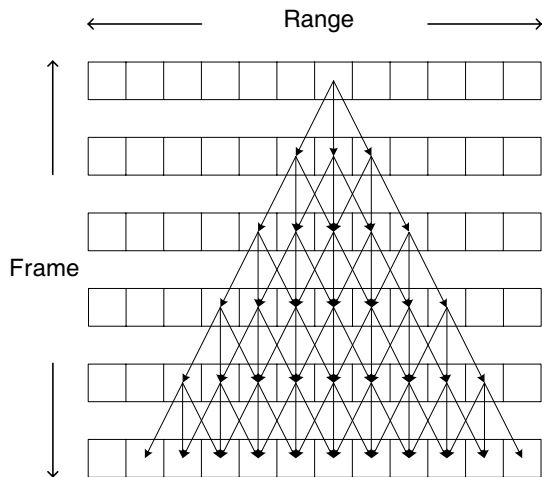


Figure 1. Potential target trajectories in multiple-scan detection.

with the searching cell number g in single scan, while it is ergodically proposed for the initial value $d(1) = \ln\Lambda(z_{l_1s_1})$. Clearly, it is seen that the detection for the moving target is changed to determine the test (22).

4. SIMULATION

Since lacking of enough real HR sea-clutter for multiple-scan detection, we are forced to employ the simulation model to handle the comparative performance analysis of the heterogeneous multiple-scan detectors, VL-HSCD, VL-HKelly and VL-HAMF, for weak target under the inhomogeneous background. And fortunately, the simulation model (especially K -distributed clutter) can be substituted for sea clutter available and convictively [19, 20].

Within the multiple-scan detection framework, the expressions of traditional single-scan detectors are as follows:

AMF detector:

$$\Lambda_{\text{AMF}}(z_{l_k s_k}) = \frac{\left| \mathbf{p}_{l_k s_k}^H \mathbf{M}_{X_{l_k s_k}}^{-1} z_{l_k s_k} \right|^2}{\mathbf{p}_{l_k s_k}^H \mathbf{M}_{X_{l_k s_k}}^{-1} \mathbf{p}_{l_k s_k}} \quad (23)$$

Kelly detector:

$$\Lambda_{\text{Kelly}}(z_{l_k s_k}) = \frac{\left| \mathbf{p}_{l_k s_k}^H \mathbf{M}_{X_{l_k s_k}}^{-1} z_{l_k s_k} \right|^2}{\left(1 + \frac{1}{K_e} z_{l_k s_k}^H \mathbf{M}_{X_{l_k s_k}}^{-1} z_{l_k s_k} \right) \left(\mathbf{p}_{l_k s_k}^H \mathbf{M}_{X_{l_k s_k}}^{-1} \mathbf{p}_{l_k s_k} \right)} \quad (24)$$

with $K_e = 20$ [27]. Precisely, the unknown $\mathbf{M}_{X_{l_k s_k}}$ is obtained with the hybrid covariance matrix estimation, and then these detectors can be renamed as HAMF detector and HKelly detector, respectively. The HKelly detector and the HSCD exhibit approximately computational complexity, while the HAMF detector achieves the relatively low complexity, and its floating-point operations (flops) is $O(N^2)$ flops less than that of the other two detectors.

Additionally, $\text{SCR}_{l_k s_k}$ as the single-scan Signal-to-Clutter Ratio (SCR) is defined as

$$\text{SCR}_{l_k s_k} = \frac{|a_{l_k s_k}|^2 \mathbf{p}_{l_k s_k}^H \mathbf{M}_{X_{l_k s_k}}^{-1} \mathbf{p}_{l_k s_k}}{\sigma_{l_k s_k}^2} \quad (25)$$

with $\sigma_{l_k s_k}^2$ is the power of clutter cell.

Therefore, the multiple-scan SCR can be obtained as

$$\text{SCR} = \sum_{k=1}^K \text{SCR}_{l_k s_k} = \sum_{k=1}^K \frac{|a_{l_k s_k}|^2 \mathbf{p}_{l_k s_k}^H \mathbf{M}_{X_{l_k s_k}}^{-1} \mathbf{p}_{l_k s_k}}{\sigma_{l_k s_k}^2} \quad (26)$$

Since the closed-form expressions for both the P_{fa} and the probability of detection (P_d) are not available, we resort to standard Monte Carlo technique. More precisely, in order to evaluate the threshold necessary to ensure a preassigned value of P_{fa} and to compute P_d , we resort to $100/P_{fa}$, $P_{fa} = 10^{-4}$, $K = 6$, $g = 5$, PRF = 1000 Hz, $N = 16$, radar resolution of 10 m, target speed of approximately 10 m/s, scanning rate of 60 rpm, $J_T \leq K$ and $J_t \geq 20$. Given P_{fa} , the threshold of multiple-scan detection also relates with the parameter K and the possible trajectory of the target in the entire surveillance scene. Hence, the drawback of the multiple-scan detection is the tremendous calculated amount while the fast algorithm is considered as the subject of future work.

Assuming that the speckle component of the generated clutter data has an exponential correlation structure covariance matrix, hence, $\mathbf{M}_{X_{l_k s_k}}$ can be expressed as

$$[\mathbf{M}_{X_{l_k s_k}}]_{ij} = \varepsilon_{l_k s_k}^{|i-j|}, \quad 0 \leq i, \quad j \leq N \quad (27)$$

where $\varepsilon_{l_k s_k}$ is the one-lag correlation coefficient. In addition, the targets are considered as Swerling 0 and Swerling 1 to adapt multiple

types of targets in real stage. Considering that the knowledge about the Radar Cross Section (RCS) of the target, related to the detection performance, may be possibly lose in some scan, the meaning of L is shown as:

- $L = 6$: It expresses that in 6 scans, the RCS information of the target is not absent across the whole searching.
- $L = 5$: It denotes that in the whole 6 scans, the RCS information of the target is missing once.

4.1. Amplitude Heterogeneity

Amplitude heterogeneity denotes the case where clutter power changes over the resolution cells due to the variation of clutter reflectivity, commonly occurred with shadowing or clutter edges. In this case, the parameters of clutter distribution, such as v and ε , are assumed to be homogeneous, and thereby the index of v or ε is dropped for brevity when the parameter of each clutter cell is no change. Then, the numerical results illustrate the detection performances of non-homogeneous multiple-detectors for two type targets under this heterogeneity.

Figures 2 and 3 show that the detection performance of the heterogeneous multiple-scan processors for Swerling 0 target (Figure 2) is slightly better than that for Swerling 1 target (Figure 3) under the same amplitude heterogeneity, where the other parameters of each clutter cell are $v = 0.4$ and $\varepsilon = 0.9$. It indicates that the fluctuating RCS of the target exhibits a little influence on multiple-scan detection. At the same time, VL-HSCD outperforms the other detectors for Swerling 0 target (about 4 dB better at $P_d = 0.9$ in Figure 2) and Swerling 1 target (about 5 dB better at $P_d = 0.9$ in Figure 3) since it is derived under the background of the compound-Gaussian model. Although in the searching process, part information of the target is absent ($L = 5$), the robust VL-HSCD also has the relatively small performance loss, compared with the other heterogeneous detectors. Additionally, when the correlation coefficient is altered, related to the PSD of the sea clutter, the detection performance is similar to that of $\varepsilon = 0.9$ and thereby is not shown in the paper.

Next, when the shape parameter of clutter increases from $v = 0.4$ to $v = 0.6$, it can be immediately seen the performance degradation of VL-HSCD in Figures 4 and 5. For HR sea clutter of K distribution, the values of shape parameter are generally observed in the region $[0.1, \infty)$ [28]. When the shape parameter is equal to infinity, the K distribution reduces to a Rayleigh distribution in amplitude, and on the contrary, it can be seen that the smaller v is, the

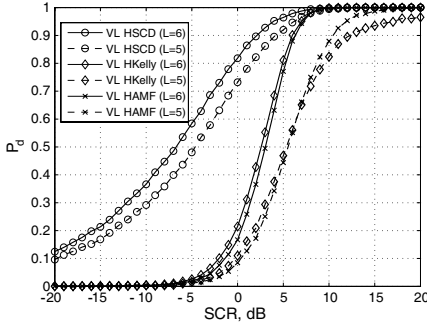


Figure 2. P_d versus SCR under amplitude heterogeneity with $v = 0.4$ and $\varepsilon = 0.9$ for Swerling 0 target.

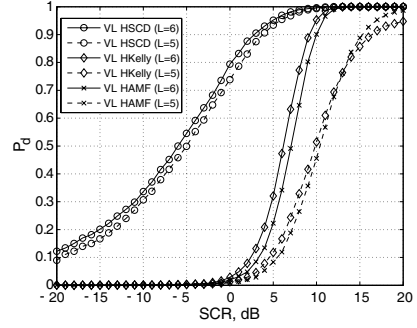


Figure 3. P_d versus SCR under amplitude heterogeneity with $v = 0.4$ and $\varepsilon = 0.9$ for Swerling 1 target.

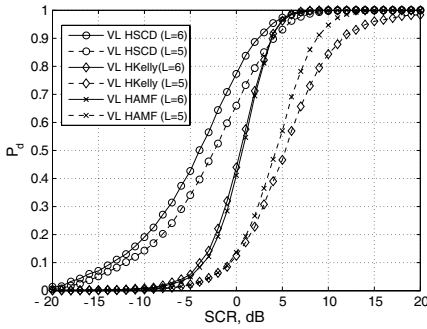


Figure 4. P_d versus SCR under amplitude heterogeneity with $v = 0.6$ and $\varepsilon = 0.9$ for Swerling 0 target.

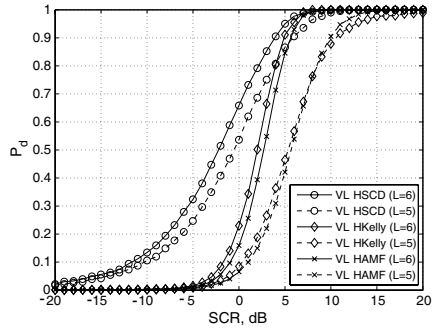


Figure 5. P_d versus SCR under amplitude heterogeneity with $v = 0.6$ and $\varepsilon = 0.9$ for Swerling 1 target.

greater difference between K distribution and Rayleigh distribution presents [29]. Additionally, U.S. Naval Research Laboratory does research on different sea-state scenarios using the HR X-band radar with vertical polarization and 0.5° beamwidth antenna in 1967. The observed results indicate that the higher sea-state is, the farther the distribution of sea clutter diverges from Rayleigh distribution. Hence, the results indicate that the VL-HSCD is more appropriate for the amplitude heterogeneity of high sea-state. The reason is that this heterogeneous multiple-scan detector is derived on the basis of the compound-Gaussian background, and thereby it suffers some

performance loss when the disturbance is close to the complex Gaussian clutter. Similarly, the performance of the VL-HSCD is better than that of the others in this case where the improvement is between about 1 and 2 dB at $P_d = 0.9$, and when the correlation coefficient is changed (such as $\varepsilon = 0.9$ to $\varepsilon = 0.95$) with the same shape parameter $v = 0.6$, there is almost no detection performance loss (not shown in the paper).

4.2. Distribution Heterogeneity

Since the test and training cells have great potential in different sea-states, we consider that the cells exhibit distinct shape parameters and unchanged correlation coefficient $\varepsilon = 0.9$, standing for one case of the distribution heterogeneity, and present the detection performance of the nonhomogeneous multiple-scan processors, shown in Figures 6 and 7. Precisely, in this case, part of the training cells show the same shape parameter as the test data and the other training cells exhibit the different parameters as the test data. As observed in Figures 6 and 7, the VL-HSCD performs at least 7 dB better at $P_d = 0.9$ than the others and achieves the least performance loss when some information of target is neglected. In the derivation of VL-HSCD, the influence of the texture component, whose PDF contains the shape and scale parameters, is involved by means of the integral operation in the expression (9), resulting in the performance superiority of this detector under the distribution heterogeneity in compound-Gaussian clutter.

Otherwise, when the shape parameter is fixed, such as $v = 0.4$, and the correlation coefficient of speckle component is changed in each

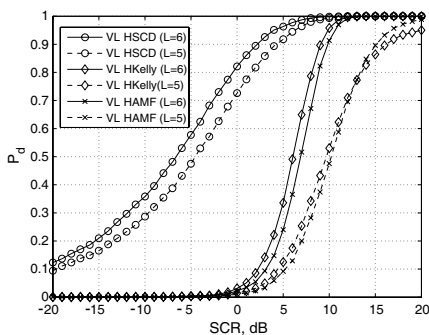


Figure 6. P_d versus SCR under distribution heterogeneity with $\varepsilon = 0.9$ for Swerling 0 target.

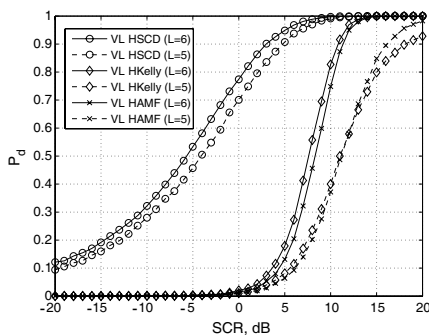


Figure 7. P_d versus SCR under distribution heterogeneity with $\varepsilon = 0.9$ for Swerling 1 target.

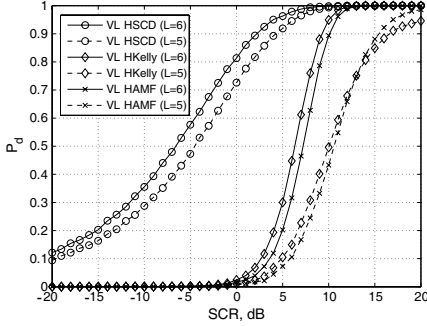


Figure 8. P_d versus SCR under distribution heterogeneity with $\nu = 0.4$ for Swerling 0 target.

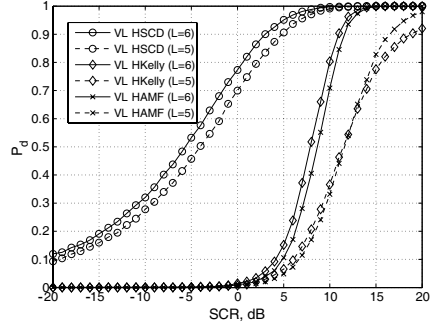


Figure 9. P_d versus SCR under distribution heterogeneity with $\nu = 0.4$ for Swerling 1 target.

cell, the detection results are shown in Figures 8 and 9, respectively. Specially, the typical values of ε for radar sea-clutter are in the range $[0.9, 0.99]$ for different conditions [23]. Figure 8 illustrates the detection performance for Swerling 0 target, while Figure 9 shows the counterpart for Swerling 1 target.

In the environment of distribution heterogeneity, the detection performance of VL-HSCD is superior to that of the others. The plots in Figures 8 and 9 show that, for $P_d = 0.9$, there exists the loss of more than 7 dB between the VL-HSCD and the other detectors. VL-HSCD is completely insensitive to the fluctuation in the value of ε , presenting the robustness to the correlation property of the sea clutter. Meanwhile, when the absence of RCS meets in the searching process, resorting to VL method, the performance degradation of all inhomogeneous detectors is not serious, representing the robustness to the searching method.

In fact, it is straightforwardly seen that the model of the sea clutter is mainly determined by the shape parameter and the correlation coefficient. Therefore, combining the cases, the adaptive heterogeneous multiple-detector, VL-HSCD, achieves the high detectability for the weak target under the various conditions of inhomogeneous clutter.

5. CONCLUSION

In this paper a framework of multiple-scan signal detection taking the clutter heterogeneity into account which plagues practical radar target detection, is presented and analyzed. For the uniformity environment, the researchers already evaluate and develop the multiple-scan

detection approaches to improve the performance of detecting the weak target in the literatures. However, considering that the clutter heterogeneity is commonly encountered in the realistic conditions, the non-homogeneous multiple-scan detectors, such as VL-HAMF, VL-HKelly and VL-HSCD, are ensured to detect the weak moving target.

Under the assumption for the different heterogeneous clutter scenarios, the detection performance of the multiple-scan detectors, VL-HAMF, VL-HKelly and VL-HSCD, are compared, and the simulation results for the performance assessment based on Monte Carlo method are presented. Specially, the detection performance of VL-HSCD proposed in the paper is remarkably superior to that of the others in both amplitude-heterogeneous and distribution-heterogeneous cases. Even when some information of target is disappeared, VL-HSCD outperforms the other detectors and achieves the robustness to VL algorithm.

ACKNOWLEDGMENT

This work has been supported by National Natural Science Foundation of China (61178068) and by Sichuan Youth Science and Technology Foundation (2011JQ0024).

REFERENCES

1. Carlson, B. D., E. D. Eva, and S. L. Wilson, "Search radar detection and track with the hough transform, Part I: System concept," *IEEE Trans. on Aerosp. Electron. Syst.*, Vol. 30, No. 1, 102–108, 1994.
2. Nichtern, O. and S. R. Rotman, "Parameter adjustment for a dynamic programming track-before-detect-based target detection algorithm," *EURASIP Journal on Advances in Signal Processing*, Vol. 2008, 2008.
3. Deng, X., Y. Pi, M. Morelande, and B. Moran, "Track-before-detect procedures for low pulse repetition frequency surveillance radars," *IEL Radar, Sonar, Navig.*, Vol. 5, No. 1, 65–73, 2011.
4. Hatam, M., A. Sheikhi, and M. A. Masnadi-Shirazi, "Target detection in pulse-train MIMO radars applying ICA algorithms," *Progress In Electromagnetics Research*, Vol. 122, 413–435, 2012.
5. Qu, Y., G. S. Liao, S. Q. Zhu, and X. Y. Liu, "Pattern synthesis of planar antenna array via convex optimization for airborne forward looking radar," *Progress In Electromagnetics Research*, Vol. 84, 1–10, 2008.

6. Qu, Y., G. Liao, S.-Q. Zhu, X.-Y. Liu, and H. Jiang, "Performance analysis of beamforming for MIMO radar," *Progress In Electromagnetics Research*, Vol. 84, 123–134, 2008.
7. Panagopoulos, S. and J. J. Soraghan, "Small-target detection in sea clutter," *IEEE Trans. on Geosci. Remote Sens.*, Vol. 42, No. 7, 1355–1361, 2004.
8. Schleher, D. C., "Periscope detection radar," *IEEE radar Conference*, 704–707, 1995.
9. McDonald, M. and S. Lycett, "Fast versus slow scan radar operation for coherent small target detection in sea clutter," *IEE Radar, Sonar, Navig.*, Vol. 152, No. 6, 429–435, 2005.
10. Carretero-Moya, J., J. Gismero-Menoyo, A. Asensio-López, and Á. Blanco-del-Campo, "Application of the Radon transform to detect small-targets in sea clutter," *IET Radar, Sonar, Navig.*, Vol. 3, No. 2, 155–166, 2009.
11. Herselman, P. L. and H. J. de Wind, "Improved covariance matrix estimation in spectrally inhomogeneous sea clutter with application to adaptive small boat detection," *IEEE radar Conference*, 94–99, 2008.
12. Besson, O., J. Y. Tournet, and S. Bidon, "Knowledge-aided Bayesian detection in heterogeneous environments," *IEEE Signal Process. Lett.*, Vol. 14, 355–358, 2007.
13. Tang, B., J. Tang, and Y. N. Peng, "Convergence rate of LSMI in amplitude heterogeneous clutter environment," *IEEE Signal Process. Lett.*, Vol. 17, No. 5, 481–484, 2010.
14. Wang, P., H. B. Li, and B. Himed, "Parametric rao tests for multichannel adaptive detection in partially homogeneous environment," *IEEE Trans. on Aerosp. Electron. Syst.*, Vol. 47, No. 3, 1850–1862, 2011.
15. Bidon, S., O. Besson, and J.-Y. Tournet, "A bayesian approach to adaptive detection in nonhomogeneous environments," *IEEE Trans. on Signal Process.*, Vol. 56, No. 1, 205–217, 2008.
16. Buzzi, S., M. Lops, L. Venturino, and M. Ferri, "Track-before-detect procedures in a multi-target environment," *IEEE Trans. on Aerosp. Electron. Syst.*, Vol. 44, No. 3, 1135–1150, 2008.
17. Viterbi, A. J., "A personal history of the Viterbi algorithm," *IEEE Signal Process. Mag.*, Vol. 23, No. 4, 120–142, 2006.
18. Swerling, P., "Radar probability of detection for some additional fluctuating target cases," *IEEE Trans. on Aerosp. Electron. Syst.*, Vol. 33, No. 2, 698–709, 1997.
19. Unsworth, C. P., M. R. Cowper, S. McLaughlin, and B. Mulgrew,

- “Re-examining the nature of radar sea clutter,” *IEE Proceedings on Rader Signal Processing*, Vol. 149, No. 3, 105–114, 2002.
20. Conte, E., A. De Maio, and C. Galdi, “Statistical analysis of real clutter at different range resolutions,” *IEEE Trans. on Aerosp. Electron. Syst.*, Vol. 40, No. 3, 903–918, 2004.
 21. Conte, E. and M. Longo, “Characterization of radar clutter as a spherically invariant random process,” *IEE Proceedings F, Communications, Radar and Signal Processing*, Vol. 134, No. 2, 191–197, 1987.
 22. Ward, K. D., J. A. Tough, and S. Watts, “Sea clutter: Scattering, the K -distribution and radar performance,” *IET Radar, Sonar and Navigation Series*, Vol. 20, 45–95, 2006.
 23. Gini, F. and M. Greco, “Covariance matrix estimation for CFAR detection in correlated heavy tailed clutter,” *Signal Processing*, Vol. 82, No. 12, 1847–1859, 2002.
 24. Aboutanios, E. and B. Mulgrew, “Hybrid detection approach for STAP in heterogeneous clutter,” *IEEE Trans. on Aerosp. Electron. Syst.*, Vol. 46, No. 3, 1021–1033, 2010.
 25. Rangaswamy, M., J. H. Michels, and B. Himed, “Statistical analysis of the non-homogeneity detector for STAP applications,” *Digital Signal Processing*, Vol. 44, No. 3, 253–267, 2004.
 26. Pulford, G. W. and B. F. La Scala, “Multihypothesis Viterbi data association: algorithm development and assessment,” *IEEE Trans. on Aerosp. Electron. Syst.*, Vol. 46, No. 2, 583–609, 2010.
 27. Kelly, E. L., “Adaptive detection in non-stationary interference, Part III,” *Tech. Rep.*, No. 761, Lincoln Lab., MIT, Lexington, 1987.
 28. Watts, S., “Radar detection prediction in K -distributed sea clutter and thermal noise,” *IEEE Trans. on Aerosp. Electron. Syst.*, Vol. 23, No. 1, 40–45, 1987.
 29. Nohara, T. J. and S. Haykin, “Canadian east coast radar trials and the K -distribution,” *IEE Proceedings F Radar and Signal Processing*, Vol. 138, No. 2, 80–88, 1991.